

Second-order interactions in a medium containing perfect-conducting hyperspherical inclusions

This article has been downloaded from IOPscience. Please scroll down to see the full text article.

2004 J. Phys. A: Math. Gen. 37 11911

(<http://iopscience.iop.org/0305-4470/37/49/010>)

View [the table of contents for this issue](#), or go to the [journal homepage](#) for more

Download details:

IP Address: 171.66.16.65

The article was downloaded on 02/06/2010 at 19:47

Please note that [terms and conditions apply](#).

Second-order interactions in a medium containing perfect-conducting hyperspherical inclusions

A Alexopoulos

Electronic Warfare and Radar Division, Defence Science and Technology Organisation,
PO Box 1500, Edinbrugh 5111, Australia

Received 23 August 2004, in final form 19 October 2004

Published 24 November 2004

Online at stacks.iop.org/JPhysA/37/11911

doi:10.1088/0305-4470/37/49/010

Abstract

We consider the interaction between two hyperspherical inclusions surrounded by a medium experiencing an \mathbf{E} -field in the perfect-conducting limit. By the use of d -dimensional dipole moments we show that the dielectric function of the medium can be calculated to any order n . In particular, $\kappa_n^{(d)}$, the coefficient of $O(c^2)$ in the series expansion for the dielectric function is determined in terms of a dimensional dependence, which even though it is mathematically complex, proves to be superior in convergence to other methods. We calculate the potential difference between the two hyperspheres for various limits, including the all important closely-packed limit. Using the theory of continued fractions, we investigate the convergence of the interaction terms between the two inclusions and obtain results that reduce the enormous number of calculations that need to be computed as $n \rightarrow \infty$. The latter may be useful in the pursuit of a theory that resums the complicated interaction terms present in the two-body + medium problem with a view towards an improved effective medium theory.

PACS numbers: 03.50.De, 41.20.Cv

1. Introduction

One of the areas of physics that has been of great interest throughout the years has been the study of non-homogeneous systems where particles or inclusions are embedded in a host medium, e.g., such as in the case of a composite material. For such systems we are interested in a variety of physical properties ranging from the electrostatic/magnetostatic behaviour, heat conduction or diffusion to elasticity and porosity effects. While these properties seem different at first glance, a close examination shows that there is a common mathematical equivalence in all of them. While the symbols change, the underlying physics is the same so that for instance in the case of a composite material we may wish to know something about

the dielectric function, which is not so different¹ from obtaining the Huggins coefficient of a fluid that has particles dissolved in it. One suitable theory that can describe these different systems has been the effective medium theory (EMT). While EMT is by no means the only theory that one can make use of, it is nevertheless one of the most successful and versatile theories around and not surprisingly, one that researchers use mostly for the solution of many physical systems. The central concept of EMT is very simple: it deals with how a single particle interacts with its surrounding medium whose effects are ‘averaged’ over the entire medium that contains n such particles. The solution to this one-body problem is an old one and dates back hundreds of years. For instance, in the study of the dielectric properties of a medium we consider an electric field \mathbf{E}_0 which acts on a particular inclusion. The idea here is to calculate the interaction of the inclusion with the medium and thus a good starting point is to obtain the local field in the vicinity of the inclusion. However, the nagging question is whether the description is microscopic, mesoscopic or macroscopic as dictated by the size of the inclusion. In 1870 Lorentz [1] investigated this issue while he was developing his ideas of macroscopic electrodynamics. Lorentz was able to compute the local field $\mathbf{E}_{\text{local}}$ acting on a particle in a medium by considering a cubic crystal made up of identical particles. Lorentz’s field was not a microscopic field nor the average field of the medium and for this and other reasons his theory received its fair share of criticism [2, 3]. What was needed in order to improve the theory was a proper connection between microscopic and macroscopic parameters. One way we can attempt to do this is to relate the dipole moment of an inclusion to the local electric field. To state this more clearly what is needed is a way to associate a macroscopic parameter such as the dielectric constant ϵ with a microscopic property, such as the particle polarizability α . The latter has been achieved in the theory that has come to be known as the Clausius–Mossotti relation [4, 5] which works well for various dielectric liquids and gases. The problem with the Clausius–Mossotti formula was the difficulty in obtaining the microscopic parameter α (polarizability) and efforts were made to obtain it using semi-classical methods such as spring models for atomic systems for example. However, the fact that α is a microscopic parameter warrants the idea that the most appropriate approach is to calculate α using a full quantum mechanical analysis [6–8]. The polarizability has been a persistent issue that has lingered around even when extensions to the Clausius–Mossotti formulation have been attempted. One such extension that deals with the case of composite materials has been the Maxwell–Garnett theory. Once again the key ingredient here is to determine the polarizability and this is done by using a classical approach whereby the inclusion has spherical geometry with dielectric constant ϵ_1 and radius a . The geometry of the inclusion is best approximated as a sphere because it is far easier to obtain analytic solutions this way, however there have been cases where the inclusions have been assumed to have non-spherical geometries such as ellipsoids for example, but such an approach involves elliptic integrals [9, 10]. The Maxwell–Garnett theory has been advanced by the work of Bruggeman [11] who has made improvements by analysing the symmetrical properties of a composite system. Bruggeman’s assumption considers a composite host of dielectric constant ϵ and a spherical inclusion of radius a embedded in it whose dielectric constant is ϵ_1 . The field that the inclusion experiences far away is taken to be constant but as we get closer to the inclusion the field varies—see [12, 8] for more details. While EMT has been applied to many non-homogeneous systems with some success it has failed to produce exact results in many other cases. The major shortcoming is due to a very simple reason as was previously stated, i.e., EMT is a one-body theory that deals with how a particle interacts with the surrounding medium. What is needed

¹ This does not imply anything about the difficulty in obtaining solutions to either of these similar systems. In general, the solution to the fluid-dynamics case is more involved than the electrostatic case but the same principles hold.

is an improvement by extending conventional EMT interactions to incorporate many-body interactions but even the two body corrections seem to be formidable in nature as we shall see later on. To gain an insight as to why we must go beyond conventional EMT consider the results for the dielectric function of a composite system in the superconducting limit $\epsilon \rightarrow \infty$. If we obtain the dielectric function via a virial expansion in the volume fraction of inclusions c , we find for spherical inclusions, that the Maxwell–Garnett theory gives the second-order coefficient κ of $O(c^2)$ as 3, while the Bruggeman theory gives the value $\kappa = 9$. The true value happens to be 4.51 but more on this later. Both the Maxwell–Garnett and Bruggeman theories are correct to first order but fail when we consider second order effects. These second order interactions are necessary if current EMT is to give much improved results for most systems under investigation. In this paper we will deal with these second-order interactions via a generalized d -dimensional method of images approach that gives all known solutions as special limiting cases. It will allow us to extend conventional EMT to incorporate two-body effects which are required if both theory and experiment are to agree more. Moreover, while many-body effects are extremely difficult to analyse, we will resum the complex interaction terms that give rise to such effects so that we are not just improving conventional one-body EMT, but are laying the foundations for the next interesting step: the study of a three-body EMT. All this will be done in the context of obtaining the dielectric function of a composite system as well as the potential difference of that system containing hyperspherical inclusions. The paper is organized in the following manner: in section 2 we discuss in more detail what our objectives are and we introduce the theory behind the method of images. In section 3 we extend the method of images to a d -dimensional form. Section 4 generalizes the d -dimensional dipoles and charges to any order n which is necessary in order to maintain the correct convergence and we obtain the d -dimensional dielectric function to second order in the volume fraction of inclusions. In section 5 we obtain the potential difference between two hyperspheres and resum the complicated terms for the case when the hyperspheres are in contact (closely packed limit) via the use of continued fractions. We do the same in section 6 but for varying separations and give asymptotic solutions derived from the resummation of the infinite series. In section 7 we discuss and interpret some of the results and conclude the paper in section 8.

2. The method of images

We are reminded that although studies have been made in order to determine thermal conduction, magnetic permeability and other effects for example, of particular interest has been the determination of the dielectric function to $O(c^2)$, where c is the volume fraction of inclusions in a medium. From this point on we will consider this type of system in our analysis. In 1873 Maxwell [13] obtained the exact $O(c)$ coefficient for the $d = 3$ case and since that time others have made similar contributions to the problem by using various techniques for both the $d = 2, 3$ cases [14, 15]. Indeed the coefficient of $O(c)$ is a relatively simple problem to deal with because as we mentioned earlier we are concerned with one inclusion interacting with the host medium and this is just conventional EMT. Matters are complicated when we consider the $O(c^2)$ coefficient because this involves two-inclusion interactions and it is of no surprise that it took about 100 years after Maxwell before a serious attempt was made at solving this problem, notably by the work of Jeffrey [16] who used a multipole expansion method in $d = 3$ to solve for κ :

$$\epsilon = \epsilon_0(1 + [\epsilon]c + \kappa c^2 + O(c^n)). \quad (1)$$

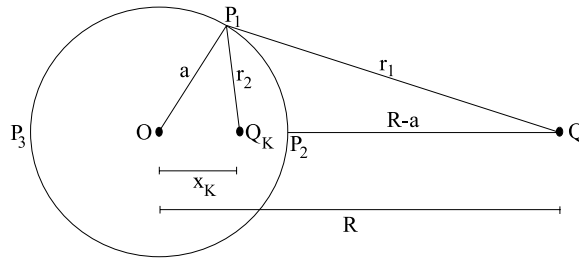


Figure 1. For a charge Q placed near an earthed sphere we can derive the first image position from the centre $b_1 = x_K$ of the image charge Q_K . By generalizing this procedure we can obtain the position of an n th order charge by the use of (19). Note that there is an absence of a dipole in this figure because the dipole moment is induced by the external electric field \mathbf{E}_0 .

The coefficient $[\varepsilon]$ in (1) is the solution due to Maxwell which we can write in d -dimensions as

$$[\varepsilon] = d\gamma \equiv \left(\frac{\varepsilon_1 - \varepsilon_0}{\varepsilon_1 + (d-1)\varepsilon_0} \right), \quad (2)$$

where γ is proportional to the polarizability of the inclusion due to the \mathbf{E} -field and $\varepsilon_1, \varepsilon_0$ are the dielectric constants of the inclusion and the host medium respectively. For the case of perfect-conducting inclusions, (2) reduces to the simple form $[\varepsilon] = d$. Our approach here will be through the use of the theory of images albeit in a more sophisticated form than usual and via an extension to d dimensions. The theory of images has been studied extensively by many over the years from as far back as when it was founded by Lord Kelvin [17]. The method has proven to be very useful in many areas of physics, from classical electrostatics, electromagnetic theory and even in the solution of quantum mechanical effects which involve forces between atoms and molecules near surfaces, the scanning tunnelling microscope (STM) being one example of the latter [18–20]. The theory of images that we are interested in using here considers the potential due to a charge Q outside a perfect conducting sphere (three-dimensional) as being equal to two other point charges. One point charge exists at the image point $x_K = \frac{a^2}{R}$ with charge $Q_K = \frac{-aQ}{R}$, while the other point charge which is equal to $-Q_K$, for an uncharged sphere, is located at the origin O . The radius of the sphere being a and the distance of the charge from the centre defined as R . Specifically if the sphere is grounded, see figure 1, we can ignore the charge $-Q_K$ at the origin. At any point P_1 along the surface of the sphere the potential is given as

$$V = \frac{1}{4\pi\varepsilon_0} \left(\frac{Q}{r_1} + \frac{Q_K}{r_2} \right). \quad (3)$$

By considering the equipotential surface of $V = 0$ through P_1 we can write (3) as

$$\frac{r_2}{r_1} = -\frac{Q_K}{Q} = \lambda. \quad (4)$$

Comparing points P_2 and P_3 we have

$$\lambda = \left(\frac{r_2}{r_1} \right) \Big|_{P_2} = \frac{a - x_K}{R - a} \quad (5)$$

and

$$\lambda = \left(\frac{r_2}{r_1} \right) \Big|_{P_3} = \frac{a + x_K}{R + a}, \quad (6)$$

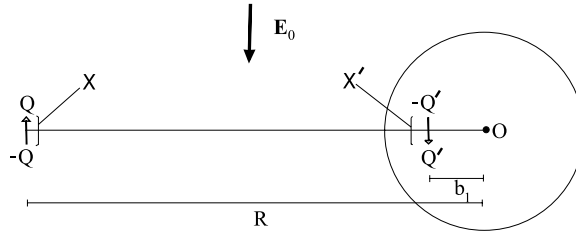


Figure 2. From the definition of a dipole, two charges are placed at infinitesimal distances apart given as x corresponding to dipole p_1 on the left and x' for the image dipole p_2 inside the sphere which exists at a distance $b_1 = Rx'/x$. O is the centre of the sphere.

respectively. By equating (5) and (6) and then multiplying them we obtain the first displacement of Q_K from the origin

$$(a - x_K)(R + a) = (a + x_K)(R - a) \Rightarrow x_K = \frac{a^2}{R} \equiv b_1 = a\omega_1. \quad (7)$$

Furthermore, from

$$\lambda = \frac{a}{R} = -\frac{Q_K}{Q} \Rightarrow Q_K = \frac{a}{R}Q \equiv \frac{b_1}{a}Q = \omega_1 Q. \quad (8)$$

It is worth noting in (7) and (8), that b_1 is the position of the first image and that any subsequent image position is given by b_j in equation (19) later on. Similarly we write the continued fraction $w_j = b_j/a$ which is obtained by (18). The problem is complicated slightly when we introduce an electric field \mathbf{E}_0 which acts in the parallel and perpendicular direction in the two-sphere system respectively. The electric field in the perpendicular direction creates dipoles and so we must map dipoles to dipoles between the spheres. On the other hand, the parallel electric field induces point dipoles *and* point charges (a residual image point charge), so that the mappings consist of point dipoles and charges being mapped to point dipoles and charges between the spheres. By definition, a dipole consists of a positive and negative charge which are an infinitesimal distance x apart and with the direction of the dipole being from the negative to the positive charge, so that $p = Qx$ where p is the dipole and Q is the charge. We will examine the point dipole for the perpendicular field case, see figure 2. A dipole p_1 created from an electric field at a distance R outside a sphere induces an image dipole inside that sphere at a separation b_1 from the origin. The dipole $p_1 = Qx$ while the image dipole is $p_2 = Q'x'$ and from figure 2 we have the ratio

$$\frac{b_1}{R} = \frac{x'}{x}. \quad (9)$$

We can now find p_2 in terms of p_1 and noting that $Q' = -Qa/R$ we have

$$p_2 = -Q \left(\frac{a}{R}\right) \frac{b_1}{R} x, \quad (10)$$

by eliminating x' . From the definition of p_1 however (10) simplifies to

$$p_2 = -p_1 \left(\frac{a}{R}\right)^3. \quad (11)$$

Equation (11) was obtained for the perpendicular field case while the parallel case is exactly the same except that the sign changes, see (14) in the next section for the d -dimensional

extension and compare to (11). From (14) we can see that the charges have been written in terms of the dipole p_1 . From figure 2

$$\begin{aligned} Q' &= -Q \left(\frac{a}{R} \right) \left(\frac{x}{R} \right) \\ &= -\frac{Q}{a} \left(\frac{a}{R} \right)^2 x, \end{aligned} \quad (12)$$

so that finally we have

$$Q' = -\frac{p_1}{a} \left(\frac{a}{R} \right)^2. \quad (13)$$

These results for $d = 3$, i.e., for spheres, form the basis of our analysis in general d dimensions in the next section. Others over time have extended these ideas to many problems. Neumann [21] for example, solved the problem of a three-dimensional dielectric sphere. In more recent times these results have been generalized [22, 23] in d -dimensional space, i.e., the spheres become *hypersurfaces* in arbitrary dimensions. In the sections to follow we derive expressions for the d -dimensional dipoles and charges and obtain a general result for the κ coefficient in (1) to any order n . Various limits are studied and compared to the results of others. One of the issues that needs to be dealt with when calculating κ is the enormous number of complex terms that arise which can be more than several hundred thousand for a typically simple calculation of small order n . An attempt has been made to resum these complex terms so that not so many terms are needed, especially since computationally we run into problems of memory and time. Such a resummation has been investigated using the convergence properties of continued fractions and is presented in the context of deriving the d -dimensional potential difference between the two hyperspheres. We present the results for the behaviour of the voltage at various limits including the closely packed limit. We start by expanding the ideas discussed so far on the theory of images in order to incorporate d -dimensional dipoles and charges and generalize them to arbitrary order n . This allows us to solve for the dielectric function of a composite system in d dimensions.

3. The d -dimensional dipoles and charges

We begin by investigating the contributions of the dipoles and the charges between the two hyperspheres—see [23] for more information on the derivation of the d -dimensional dipoles and charges. The effect of the parallel component of the electric field will be considered for brevity reasons although the perpendicular case is slightly more involved but otherwise straightforward. Figure 3 defines the first few generations of dipoles and charges that will form the basis of the mappings between the two d -dimensional inclusions. Djordjević *et al* [24] have shown that these mappings consist of continued fractions but their solutions are for two-dimensional point dipoles *only*, a result that is exact for $d = 2$. In what follows we will not only generalize to the case of arbitrary dimensions, but we will include the contributions of the charges which vanish in the limit $d = 2$, naturally recovering the results of Djordjević *et al*. By examining figure 3, we see that the electric field in the parallel direction induces a dipole p_1 on the left hypersphere at the origin O . On the second hypersphere a dipole p_2 and charge Q_2 are generated at a distance away from the origin given by the variable b_{j-1} . Charge conservation requires that another charge $-Q_2$ of equal and opposite magnitude be created at the origin. On the third generation, the point dipole p_3 and the corresponding charges are created on the first hypersphere. These mappings of the point dipoles and charges between the hyperspheres continues infinitely from one to the other. The symmetry of the system, i.e., the hyperspheres have equal radii, means that the procedure is repeated twice to account

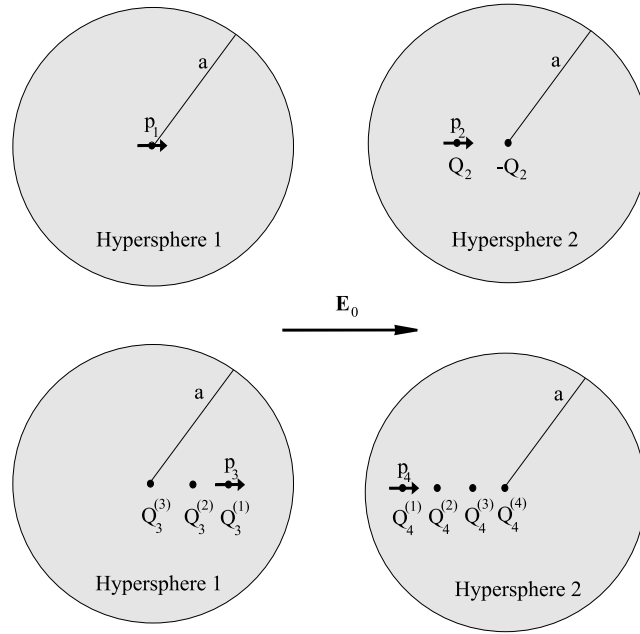


Figure 3. The dipole and charge distributions are shown here for the parallel component of the electric field. The sequence of point dipole and charge images for each generation is shown up to \mathbf{p}_4^{\parallel} , with the perpendicular distribution being analogous to the parallel case, the only major difference being the absence of the charges in the former. The superscript j in Q_n^j refers to the image point b_{j-1} (see (19)) which gives the position of the charges/dipoles as represented by the dots while n refers to the generation (or order) \mathbf{p}_n .

for the interaction of the second inclusion onto the first. On the basis of the above method and the results we have derived in the previous section for $d = 3$ we can write down the second generation point dipole p_2 and the corresponding charges as

$$\begin{aligned} p_2 &= p_1 \left(\frac{a}{R}\right)^d & Q_2^{(2)} &= -(d-2) \left(\frac{p_1}{a}\right) \left(\frac{a}{R}\right)^{d-1} \\ Q_2^{(1)} &= (d-2) \left(\frac{p_1}{a}\right) \left(\frac{a}{R}\right)^{d-1}, \end{aligned} \quad (14)$$

where (14) are the initial conditions of the system and thus the total dipole moment p_2^{tot} becomes

$$p_2^{\text{tot}} = p_2 - b_1 Q_2^{(2)} = p_1 (d-1) \left(\frac{a}{R}\right)^d. \quad (15)$$

On the third generation, we can use (14) in the derivation of p_3 and the charges to obtain

$$\begin{aligned} p_3 &= p_1 \left(\frac{a}{R}\right)^d \left(\frac{a}{R-b_1}\right)^d \\ Q_3^{(3)} &= (d-2) \left(\frac{p_1}{a}\right) \left(\frac{a}{R}\right)^{d-2} \left(\frac{a}{R-b_1}\right)^{d-1} \\ Q_3^{(2)} &= -(d-2) \left(\frac{p_1}{a}\right) \left(\frac{a}{R}\right)^{d-2} \left(\frac{a}{R}\right)^{d-1} \\ Q_3^{(1)} &= (d-2) \left(\frac{p_1}{a}\right) \left(\frac{a}{R}\right)^{d-2} \left[\left(\frac{a}{R-b_1}\right)^{d-1} - \left(\frac{a}{R}\right)^{d-2} \right], \end{aligned} \quad (16)$$

with the total dipole moment $p_3^{\text{tot}} = p_3 + Q_3^{(3)}b_2 + Q_3^{(2)}b_1$ given as

$$p_3^{\text{tot}} = p_1 \left(\frac{a}{R}\right)^d (d-1) \left(\frac{a}{R-b_1}\right)^d + p_1 \left(\frac{a}{R}\right)^d (d-2) \left[\left(\frac{a}{R-b_1}\right)^{d-1} \left(\frac{R}{a}\right) - \left(\frac{a}{R}\right)^{d-2} \right]. \quad (17)$$

Equation (17) is indicative of the fact that calculation of higher-order terms is very complicated since the number of terms that are needed becomes enormous. As previously mentioned, even for small orders in n , at least several hundred thousand terms are required in order to determine say, κ in (1). The form of these expressions is so formidable that as $n \rightarrow \infty$ it is very hard to keep track of the mappings between the hyperspheres. Fortunately in the next section we will derive these expressions as analytic/closed-form equations.

4. Higher-order dipole moments

From (17) we see that all terms involve the ratio $\omega = a/R$ and the position of the images b_j . From these results it is easy to obtain the recurrence relation for ω_j as follows [23, 24],

$$\omega_j = \frac{a}{(R - b_{j-1})}, \quad (18)$$

while in the case of b_j the recurrence relation becomes

$$b_j = \frac{a^2}{(R - b_{j-1})}, \quad (19)$$

where we note that $b_j = a\omega_j$. The dimensional dependence of the dipole terms takes the following form for $n \geq 2$:

$$p_n = p_{n-1} \left(\frac{a}{R - b_{n-2}}\right)^d. \quad (20)$$

As we shall see later, the behaviour of ω_j and b_{j-1} in the equations above needs to be investigated further as far as their convergence properties are concerned since we want to attempt a resummation of a large number of terms that involve these continued fractions. For now we want to obtain the dielectric function for hyperspherical inclusions in the perfect-conducting limit using the virial expansion to $O(c^2)$ in the low volume fraction of inclusions limit:

$$\frac{\varepsilon}{\varepsilon_0} = 1 + dc + \left(d + \frac{d}{p_1 a^d} \int_{2a}^{\infty} dR R^{d-1} \bar{p}_n^{(d)} \right) c^2 + O(c^n). \quad (21)$$

As can be seen from (21), κ has a dimensional dependence and can be calculated to any order n , that is,

$$\kappa_n^{(d)} = d + \frac{d}{p_1 a^d} \int_{2a}^{\infty} dR R^{d-1} [\bar{p}_n^{(d)}], \quad (22)$$

where $\bar{p}_n^{(d)}$ is defined below. Before doing so it is worth pointing out that by a similar routine we can calculate the expression for the perpendicular field case so that overall the total averaged dipole moment to any order is given by

$$\bar{p}_n = p_n^{\parallel \text{tot}} + (d-1)p_n^{\perp \text{tot}}, \quad (23)$$

for both the parallel and perpendicular contributions of the field or more specifically

$$\bar{p}_n^{(d)} = p_1 [1 + (d-1)(-1)^{n-1}] \prod_{i=1}^{n-1} \omega_i^d + (-1)^{n-1} (d-2) \sum_{j=2}^n Q_n^{(j)} b_{j-1}. \quad (24)$$

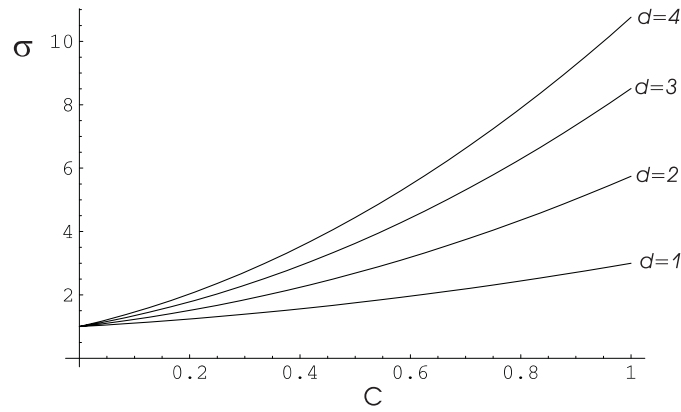


Figure 4. The conductance $\sigma = \epsilon/\epsilon_0$ has been plotted for $d = 1, 2, 3, 4$ in the low volume fraction of inclusions c , for two interacting inclusions in a host medium.

The non-trivial contributions of the line charges for each successive generation in (24) are given as

$$Q_n^{(n)} = (-1)^{n-1} \left(\frac{P_1}{a}\right) \omega_{n-1}^{d-1} \prod_{i=1}^{n-2} \omega_i^{d-2}, \tag{25}$$

for $j = n$ while for the other charge contributions we have

$$Q_n^{(j)} = -Q_{n-1}^{(j-1)} \omega_{j-1}^{d-2}, \tag{26}$$

for $n > j > 1$. The line-charges that ‘couple’ with the dipoles are determined by

$$Q_n^{(1)} = -\sum_{j=2}^n Q_n^{(j)}, \tag{27}$$

where $n > 2$. We can now write down the dimensionally dependent coefficient κ in the series for the dielectric function $\epsilon/\epsilon_0 = (1 + dc + \kappa_n^{(d)} c^2 + \dots)$, as

$$\begin{aligned} \kappa_n^{(d)} = d + \frac{d}{p_1 a^d} \int_{2a}^{\infty} R^{d-1} \left\{ p_1 [1 + (d-1)(-1)^{n-1}] \prod_{i=1}^{n-1} \omega_i^d \right. \\ \left. + (-1)^{n-1} (d-2) \sum_{j=2}^n Q_n^{(j)} b_{j-1} \right\} dR. \end{aligned} \tag{28}$$

Recalling that $\omega = a/R$, it is easy to substitute ω in (28) so that the integral is performed over ω in the interval $[0, 1/2]$ (see results of table 1). Equation (28) is the generalized d -dimensional coefficient κ that can be used to solve for any order n . This in turn allows us to calculate the d -dimensional conductance, see figure 4. In the next section we shall use these results to study the problem of the potential difference between two hyperspheres.

5. The potential difference between two hyperspheres

The problem of finding the potential difference (or voltage) and therefore capacitance between two inclusions has been of great interest. In the case where the inclusions are spheres, considerable work has been undertaken to calculate special cases of the electrostatics of such

Table 1. Values for $\kappa_n^{(d)}$ using higher-order dipole images in d dimensions. Values up to $n = 23$ are shown for $d = 2, 3$ and 4 . Note that for the case $d = 1$, $\kappa_n^{(1)} = 1$ to all orders in n . One can see from the results below that the convergence towards the known values is relatively fast given the complexity of the terms that are calculated for each order. Known values: $d = 2$, $\kappa = 2.744\,989\dots$ [24], $d = 3$, $\kappa = 4.51\dots$ [16].

$\kappa_n^{(d)}$	$d = 2$	$d = 3$	$d = 4$
$\kappa_3^{(d)}$	2.666 666	4.166 666	5.370 370
$\kappa_4^{(d)}$	2.666 666	4.291 666	5.550 925
$\kappa_5^{(d)}$	2.722 340	4.394 103	5.652 564
$\kappa_6^{(d)}$	2.722 340	4.427 576	5.691 469
$\kappa_7^{(d)}$	2.735 509	4.455 031	5.716 301
$\kappa_8^{(d)}$	2.735 509	4.468 273	5.729 623
$\kappa_9^{(d)}$	2.740 152	4.479 289	5.738 861
$\kappa_{10}^{(d)}$	2.740 152	4.485 755	5.744 690
$\kappa_{11}^{(d)}$	2.742 195	4.491 220	5.748 973
$\kappa_{12}^{(d)}$	2.742 195	4.494 825	5.751 943
$\kappa_{13}^{(d)}$	2.743 231	4.497 916	5.754 221
$\kappa_{14}^{(d)}$	2.743 231	4.500 118	5.755 901
$\kappa_{15}^{(d)}$	2.743 812	4.502 030	5.757 231
$\kappa_{16}^{(d)}$	2.743 812	4.503 469	5.758 257
$\kappa_{17}^{(d)}$	2.744 163	4.504 731	5.759 089
$\kappa_{18}^{(d)}$	2.744 163	4.505 717	5.759 751
$\kappa_{19}^{(d)}$	2.744 387	4.506 592	5.760 299
$\kappa_{20}^{(d)}$	2.744 387	4.507 297	5.760 747
$\kappa_{21}^{(d)}$	2.744 536	4.507 927	5.761 124
$\kappa_{22}^{(d)}$	2.744 536	4.508 447	5.761 438
$\kappa_{23}^{(d)}$	2.744 640	4.508 915	5.761 706

spherical pairs. Calculations have been made of the capacity of touching unequal metallic spheres [25], while extensions to this method have been used to study non-touching spheres under a variety of conditions [26]. In addition to calculations of the capacity, the total charge between two spheres and the electrostatic force, consideration has been made of dielectric sphere pairs in uniform external fields using a Green's-function technique for difference equations [27]. Various limits have been investigated and the asymptotic behaviour of both separated conducting spheres and touching dielectric spheres have been proposed [28]. Most of the work mentioned above was done using field expansions in curvilinear coordinates, such as bispherical coordinates [29]. An interesting extension of the work done so far would be to actually solve for the dielectric function using d -dimensional bispherical coordinates. In the case of a composite system, we are interested in such things as the dielectric and conductive properties. These coefficients of interest can be obtained from knowledge of the induced moments on the inclusions. Most methods lead to an infinite matrix equation, which must be truncated and inverted numerically to obtain the multipole moments. When the inclusions are close to touching, the number of multipole moments that need to be retained for an accurate solution makes numerical inversion impractical. A method for calculating the influence exerted between nearest-neighbour inclusions explicitly, that is without numerical inversion, and thus

providing an estimate of the induced multipoles of all orders, would simplify the calculation of effective properties of closely-packed composites. The method of images that has been presented in this paper might be able to help us in this context, by allowing us to gain valuable insight into the problem. Thus we will use the results that we have obtained in the previous sections to calculate the d -dimensional voltage ΔV , between two inclusions. We will derive an expression for the d -dimensional voltage using the method of images by firstly considering the contributions due to the point dipoles only, an exact result for $d = 2$ and in agreement with Djordjević *et al* [24], and then the full contributions that include the charges too. The special limit when the hyperspheres touch, $\omega = a/R = 1/2$, will be investigated due to the importance of nearest neighbour effects in closely-packed composites. As we shall see, for the case $d = 3$ when the limit of $\omega \rightarrow 1/2$ (spheres touching), the convergence is so slow that in order to converge to the expected $V \rightarrow 0$ limit an enormous (approaching infinity) number of both dipole and charge contributions need to be calculated. Fortunately, as we shall see later, we can derive expressions that reduce the large number of terms that are needed in order to calculate the potential difference between the hyperspheres. Before that however, we will investigate the full contributions due to the point dipoles and charges in the next section.

5.1. Dipole contributions

We consider two inclusions in the presence of a parallel and perpendicular component of an electric field \mathbf{E}_0 . We can write the voltage ΔV between the hyperspheres as

$$\Delta V = E_0 R + 2 \sum_{n=2}^{\infty} V_n^D, \quad (29)$$

where the factor 2 in (29) represents the effect of the other hypersphere (by symmetry) and V_n^D is the contribution from all the dipoles *only*. Here R is the separation of the centres of the two hyperspheres each of radius a . We recall from previous sections that the positions of the dipoles (charges) are given by b_n , such that

$$b_n = \frac{a\omega}{1 - \omega\omega_{n-1}}, \quad (30)$$

and each dipole p_n is generated from the previous mapping as can be seen from the following expression:

$$p_n = p_{n-1} \frac{\omega^d}{(1 - \omega\omega_{n-2})^d}. \quad (31)$$

Once again we can see that (30) can be written as $b_n = a\omega_n$ because all the ω are generated by the continued fraction

$$\omega_n = \frac{\omega}{1 - \omega\omega_{n-1}}. \quad (32)$$

We can now write down the point-dipole-only contribution to the voltage (29) as

$$V_n^D = -\frac{1}{\Omega_d} \frac{b_{n-1}^{d-1}}{a^{2(d-1)}} p_{n-1}, \quad (33)$$

where a is the radius of each hypersphere and we use (30) and (31) to solve for ΔV :

$$\Delta V = E_0 R + 2 \sum_{n=2}^{\infty} \left[-\frac{1}{\Omega_d} \frac{b_{n-1}^{d-1}}{a^{2(d-1)}} p_{n-1} \right]. \quad (34)$$

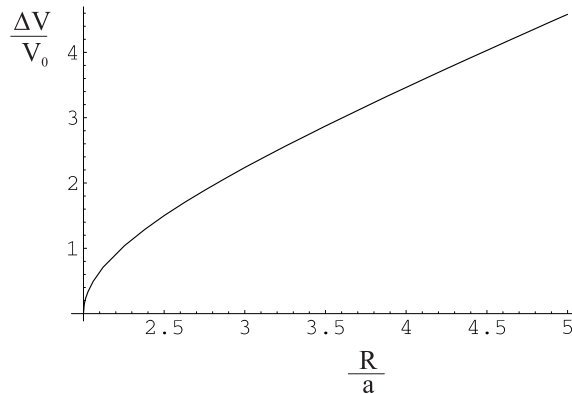


Figure 5. The voltage between two inclusions is shown for $d = 2$. Three results are actually shown (i) the result as obtained in this paper, (40), (ii) the approximation (73) and (iii) the case of Djordjević *et al* [24]. All the curves are exact and so lie on top of each other.

Before proceeding any further, we will examine (33) for the case $d = 2$ and study the all important leading terms. We will consider the leading terms given by $n = 2, 3, 4$ and note that $p_1 = \Omega_d E_0 a^d$ and $\Omega_d = 2^{d-1} \pi$. For $n = 2$, since $n = 1$ means that $V_1 = 0$, we have

$$V_2^D = -\frac{1}{\Omega_2} \frac{b_1}{a^2} p_1 \quad b_1 = \frac{a^2}{R} \quad \Omega_2 = 2\pi,$$

so that

$$V_2^D = -\frac{1}{2\pi} \frac{p_1}{R}. \quad (35)$$

In a similar way we consider the $n = 3$ case and keep in mind that $\omega_0 = 0$ and $\omega_1 = \omega = a/R$:

$$V_3^D = -\frac{1}{2\pi} \frac{b_2}{a^2} p_2 \quad b_2 = \frac{a\omega}{1-\omega^2} \quad p_2 = p_1 \omega^2, \quad V_3^D = -\frac{1}{2\pi a} \frac{\omega}{(1-\omega^2)} p_2.$$

By not writing out p_2 explicitly and after simplifying we finally have

$$V_3^D = -\frac{1}{2\pi} \frac{p_2}{(R - a^2/R)}. \quad (36)$$

The fourth-order term $n = 4$ can be expanded in the same way as before so that the following expressions are obtained:

$$V_4^D = -\frac{1}{2\pi} \frac{b_3}{a^2} p_3 \quad b_3 = \frac{a^2}{R - \frac{a^2}{R - \frac{a^2}{R}}} \quad p_3 = p_2 \frac{\omega^2}{(1-\omega^2)^2}$$

$$\omega_1 = \frac{a}{R} \quad \omega_2 = \frac{\omega}{1-\omega^2} \quad \omega_3 = \frac{\omega}{1 - \frac{\omega^2}{1-\omega^2}},$$

so that after all the ω have been replaced we arrive at the final result

$$V_4^D = -\frac{1}{2\pi} \frac{p_3}{\left(R - \frac{a^2}{R - \frac{a^2}{R}}\right)}. \quad (37)$$

The terms given by (35), (36) and (37) are exactly the same as equation (30) of the paper by Djordjević *et al* [24]. In fact this is more apparent when we plot ΔV as a function of $\bar{\omega} = R/a$, showing the exact correlation to the result obtained by Djordjević *et al* [24], who determined

Table 2. Values obtained for ΔV showing very slow convergence for $d = 3$. The first four rows show convergence due to dipole-only interactions in (40), while the last two rows include the image contributions also.

n	ΔV
10	1.299 54
20	1.292 33
150	1.289 91
200	1.289 89
10	1.246 03
20	1.244 08

their version using hyperbolic series. The reason why (34) is exact in two dimensions is because the only contributions that exist are those that come from the point dipoles. For the case $d = 2$ all charge contributions vanish. However for other dimensions, the charges do not cancel so that we need to consider these in the next section.

5.2. Dipole and charge contributions

In two dimensions we expect the charges to disappear and the only contribution to the voltage comes from the point dipoles only. The expression for the latter can be used for the case $d = 3$, but the convergence is very slow especially when we consider the limit where the spheres are touching ($\omega = 1/2$). By the methods used previously and using the results for the charges, (25), (26) and (27), we write down the expression for the charge contributions, V_n^C :

$$V_n^C = -\frac{1}{\Omega_d} \sum_{k=1}^n \frac{Q_n^{(k)}}{\rho_{k-1}^{d-2}}, \tag{38}$$

where all symbols, b, a, p and so on, have the usual meaning as encountered before. We define the parameter ρ such that

$$\rho_{k-1}^{d-2} \equiv [R - b_{k-1}]^{d-2}. \tag{39}$$

As can be seen from (39), when $d = 2, \rho = 1$ and the charges in (38) cancel each other out. Thus the total voltage ΔV , which includes both point dipoles and charges can be written as

$$\frac{\Delta V}{E_0 a} = \left(\frac{R}{a}\right) + \left(\frac{2}{E_0 a \Omega_d}\right) \sum_{n=2}^{\infty} \left[\sum_{k=1}^n \frac{Q_n^{(k)}}{\rho_{k-1}^{d-2}} - \frac{b_{n-1}^{d-1}}{a^{2(d-1)}} p_{n-1} \right]. \tag{40}$$

In two dimensions, because the charge contributions vanish, the results are exact and the potential difference between the inclusions varies as shown in figure 5. For three dimensions where the inclusions are spheres, (40) gives us an improvement in convergence in the limit when the two spheres approach each other ($\omega \rightarrow 1/2$), as compared to when we consider the point dipole contributions only. The better convergence is due to the participation of the charges but unfortunately (40) converges so slowly overall as $\omega \rightarrow 1/2$ that in order to improve upon this convergence an enormous number of terms needs to be considered which makes the whole procedure computationally difficult, see table 2. Even so the method gives us a very powerful insight that could be used in conjunction with analytical methods to resum the terms appearing in say, the continued fractions, thus giving us the desired convergence without having to compute a vast amount of terms. While such a resummation needs to be

studied carefully and in a lot more detail, something that is beyond the scope of this paper, we will nevertheless illustrate the principle by considering the limit when the hyperspheres are touching, $\omega = 1/2$ or $\Delta V = 0$.² To study the limit when the two hyperspheres touch, i.e., when $\omega = 1/2$ (or $\bar{\omega} = 2$), we will consider the continued fraction w_n (see the appendix). We notice that for any large ω such that $n \rightarrow \infty$, the continued fraction has the form

$$\omega_\infty = \frac{\omega}{1 - \frac{\omega^2}{1 - \frac{\omega^2}{1 - \frac{\omega^2}{\ddots}}}} \quad (41)$$

where for reasons we have talked about before, we are able to write such a continued fraction in ω alone. By evaluating such continued fractions at $\omega = 1/2$ we notice that we obtain the following pattern:

$$\{\omega_1, \omega_2, \omega_3, \omega_4, \dots\} = \left\{ \frac{1}{2}, \frac{2}{3}, \frac{3}{4}, \frac{4}{5}, \dots \right\}. \quad (42)$$

Now for any number x , we can expand it in a continued-fraction form such that

$$x = a_0 + \frac{1}{a_1 + \frac{1}{a_2 + \frac{1}{a_3 + \dots}}},$$

which can be represented in the following notation:

$$x = \{a_0, a_1, a_2, a_3, \dots\}.$$

From (42) we can surmise that for any w_n as $n \rightarrow \infty$, we obtain the formula

$$\omega_n = \{0, 1, n\} = \frac{1}{1 + \frac{1}{n}}, \quad (43)$$

so that by substituting values for n we derive

$$\begin{aligned} \omega_1 &= \{0, 1, 1\} = \frac{1}{1 + \frac{1}{1}} = \frac{1}{2}, \\ \omega_2 &= \{0, 1, 2\} = \frac{1}{1 + \frac{1}{2}} = \frac{2}{3}, \\ \omega_3 &= \{0, 1, 3\} = \frac{1}{1 + \frac{1}{3}} = \frac{3}{4}, \\ \omega_4 &= \{0, 1, 4\} = \frac{1}{1 + \frac{1}{4}} = \frac{4}{5}, \\ &\vdots \end{aligned} \quad (44)$$

and so forth. Thus to all orders in n , we can generate the ω in the simple form

$$\omega_n = \frac{n}{n+1}. \quad (45)$$

As the number of terms that need to be calculated increases considerably as the hyperspheres touch, (45) reduces the otherwise complex terms to a form that is computationally more

² If we were to plot (40) as a function of $\omega^{-1} = \bar{\omega} = R/a$, we find that when $\bar{\omega} = 2$, $\Delta V = 0$.

efficient. At the same time (45) gives us an idea as to how the voltage ΔV behaves at that limit. By taking the voltage due to the point dipoles only for brevity³, we can express it as

$$V_{n+2}^D = -\frac{1}{\Omega_d} \frac{b_{n+1}^{d-1}}{a^{2(d-1)}} p_{n+1}, \tag{46}$$

where we note that $n \geq 0$ and $p_1 = p_0 = \Omega_d E_0 a^d$. The dipoles are now obtained from

$$p_{n+1} = p_n \left[\frac{n}{n+1} \right]^d, \tag{47}$$

while the positions of the dipoles are given by

$$b_{n+1} = \frac{a(n+1)}{n+2}, \tag{48}$$

and by substituting (47) and (48) into (46) we obtain

$$V_{n+2}^D = -\frac{1}{\Omega_d} \left[\frac{n+1}{a(n+2)} \right]^{d-1} \left[\frac{n}{n+1} \right]^d p_{n+1}. \tag{49}$$

When we take the limit $n \rightarrow \infty$ we see that (49) simplifies to

$$\lim_{n \rightarrow \infty} V_{n+2}^D \equiv V_\infty^D = -\frac{1}{\Omega_d} \left[\frac{1}{a} \right]^{d-1} p_{\infty+1} \tag{50}$$

where we notice from (47) that $p_{\infty+1} = p_\infty$ as $n \rightarrow \infty$. This means that $p_\infty \dots p_{100} = p_{99}, p_{99} = p_{98}, p_{98} = p_{97} \dots p_1$. Equation (50) now becomes

$$V_\infty^D = -\frac{1}{\Omega_d} \left[\frac{1}{a} \right]^{d-1} p_1. \tag{51}$$

Substituting $p_1 = \Omega_d E_0 a^d$ we finally obtain

$$\frac{\Delta V}{V_0} = 2 + \frac{2}{V_0} \left(-\frac{1}{\Omega_d} \left[\frac{1}{a} \right]^{d-1} \Omega_d a^d E_0 \right) = 0, \tag{52}$$

where $V_0 = E_0 a$. Remarkably we see that for inclusions of any dimension d , the voltage ΔV becomes zero at $\omega = 1/2$, as expected.

6. The convergence of the potential difference for varying separations

In the previous section we have considered the special limit when the hyperspheres are touching, i.e., $\omega = a/R = 1/2$ (or $\bar{\omega} = R/a = 2$). Equation (45) has reduced the enormous number of terms that would usually be required for the closely-packed limit. Unfortunately, for other hyperspherical separations such as $\omega \in [\frac{1}{3}, \frac{1}{4}, \frac{1}{5}, \frac{1}{6}, \dots]$, a similar form to (45) is not possible because the convergence of the ω varies dramatically for different separations. However, a close study of the convergence of the ω_n for these different separations shows that only the first few orders vary significantly, while higher orders of ω converge to a constant value which we shall call β . We define an order γ which is chosen as the maximum number of terms that need to be calculated in ω_n before the convergence becomes constant. Typically, γ is chosen after calculating the order up to $n = 6$ or $n = 7$ in ω_n and so $\gamma = 6$ or 7 respectively. If we choose $\gamma < 6$ say, we encounter convergence problems and we must evaluate all orders by the brute force calculation/analysis of the continued fractions. In fact the values of $\beta(\omega)$

³ The same can be done with the voltage due to the charges, V_n^C , but it is more involved.

Table 3. Saturated convergence values of $\beta(\omega|n > \gamma)$ for various selected hyperspherical separations.

$\omega = a/R$	β
$\frac{1}{3}$	$\frac{76910}{201353}$
$\frac{1}{4}$	$\frac{7865521}{29354524}$
$\frac{1}{5}$	$\frac{6665999}{31938720}$
$\frac{1}{6}$	$\frac{7997214}{46611179}$
$\frac{1}{7}$	$\frac{4976784}{34111385}$
$\frac{1}{8}$	$\frac{1905632}{15003009}$
$\frac{1}{9}$	$\frac{4435929}{39424240}$
$\frac{1}{10}$	$\frac{950599}{9409960}$

are determined from the study of the limits of the continued fractions of ω_n , for $n \geq \gamma$, for all separations. For example we obtain for $\omega = 1/3$ and $\omega = 1/4$ respectively:

$$\beta\left(\frac{1}{3}\right) = \left\{0, 2, \overset{\{15\}}{1}, 2, 14, 2\right\} = \frac{76910}{201353}, \quad (53)$$

and

$$\beta\left(\frac{1}{4}\right) = \left\{0, 3, 1, \overset{\{12\}}{2}, 1\right\} = \frac{7865521}{29354524}, \quad (54)$$

and so on. The notation $\overset{\{15\}}{1}$ means that the number 1 is repeated thereafter another 14 times and likewise the pair term $\overset{\{12\}}{2}$ is repeated 11 times. Table 3 shows values of β for typical separations $\omega = a/R$. We now return to the expression for the voltage between two hyperspheres in the dipole only contribution limit for brevity, and rewrite it in the following form:

$$\frac{\Delta V}{V_0} = \frac{R}{a} - \left(\frac{2}{V_0 \Omega_d a^{d-1}}\right) \left[2^{d-1} \pi E_0 a^d \omega_1^{d-1} + \sum_{n=2}^{\infty} \omega_n^{d-1} p_n\right]. \quad (55)$$

After the first few orders, i.e., when $n \geq \gamma$, the ω converge to the values given by $\beta(\omega)$ —see table 3 for some representative values. The second term in equation (55) can be written as

$$\sum_{n=2}^{\infty} \omega_n^{d-1} p_n = \sum_{n=2}^{\gamma} \omega_n^{d-1} p_n + \sum_{n=\gamma+1}^{\infty} \omega_n^{d-1} p_n. \quad (56)$$

The third term in (56) can be truncated to N , as $N \rightarrow \infty$, such that the required convergence is established, thus we have

$$\sum_{n=\gamma+1}^N \omega_n^{d-1} p_n = \omega_{\gamma+1}^{d-1} p_{\gamma+1} + \omega_{\gamma+2}^{d-1} p_{\gamma+2} + \cdots + \omega_N^{d-1} p_N. \quad (57)$$

Since $n = \gamma + 1$ implies that we are considering the ω whose values converge to $\beta(\omega)$, (57) can be expressed as

$$\sum_{n=\gamma+1}^N \omega_n^{d-1} p_n = \beta^{d-1}(\omega)[p_{\gamma+1} + p_{\gamma+2} + \cdots + p_N], \quad (58)$$

where $p_{\gamma+1}, p_{\gamma+2}, \dots$ are obtained from

$$p_n = 2^{d-1} \pi E_0 a^d \prod_{k=1}^{n-1} \omega_k^d. \tag{59}$$

Using (59), we can further write (57) in the form

$$\sum_{n=\gamma+1}^N \omega_n^{d-1} p_n = 2^{d-1} \pi E_0 a^d \beta^{d-1}(\omega) \prod_{k=1}^{\gamma} \omega_k^d \left[1 + \omega_{\gamma+1}^d + \prod_{k=\gamma+1}^{\gamma+2} \omega_k^d + \dots + \prod_{k=\gamma+1}^{N-1} \omega_k^d \right], \tag{60}$$

so that we finally obtain

$$\sum_{n=\gamma+1}^N \omega_n^{d-1} p_n = 2^{d-1} \pi E_0 a^d \beta^{d-1}(\omega) \prod_{k=1}^{\gamma} \omega_k^d \left[1 + \sum_{j=1}^{N-\gamma-1} \beta^{jd}(\omega) \right]. \tag{61}$$

Equation (61) reduces the number of calculations that are needed to calculate the potential difference because only the first few orders are computed, up to γ , while all other terms are factored in as constants in the form of all the β . Substituting (61) into (55) we obtain the final form for the potential difference ΔV as given by (65). Equation (65) allows us to work out the potential difference between two hyperspheres at separations $\omega = a/R$ (or $\bar{\omega} = R/a$): $\omega \in [\frac{1}{2}, \frac{1}{3}, \frac{1}{4}, \frac{1}{5}, \dots]$ for instance without the need to resort to an enormous number of terms (approaching infinity), in order to obtain the required convergence for the d -dimensional voltage. From (61), the sum is truncated to N but ideally we expect that $N \rightarrow \infty$. However, as $N \rightarrow \infty$ in (61), $\beta(\omega) \rightarrow 0$ since only the first few terms contribute to the sum

$$\sum_{j=1}^{N-\gamma-1} \beta^{jd}(\omega) = \beta^d(\omega) + \beta^{2d}(\omega) + \dots + \beta^{(N-\gamma-1)d}(\omega). \tag{62}$$

Suppose we consider $\beta(\omega) \geq \omega_{\gamma+1}$ with $\gamma = 7$ say, to be $\beta(1/3) = 0.381\ 966$ then from (62) we have (let $d = 2$ for simplicity)

$$\sum_{j=1}^{N-8} \beta^{2j}(\omega) = (0.381\ 966)^2 + (0.381\ 966)^4 + \dots + (0.381\ 966)^{(2N-16)}. \tag{63}$$

We find that each successive power makes β smaller and smaller so that only the leading terms can be retained. To a very good approximation we can write the sum as

$$\sum_{j=1}^{N-\gamma-1} \beta^{jd} \rightarrow \sum_{j=1}^{\gamma} \beta^{jd}. \tag{64}$$

Thus from (65) we see that only the leading terms can be used up to γ , without the need to calculate an infinite number of terms which means that (65) can be considered as a resummation of the infinite series. The results of (65) are very accurate as can be seen by figures 7 and 8 for inclusions of $d = 2$ and 3 respectively. From figure 7 for the $d = 2$ case, there are three curves given by (40), (73) and (65). All three methods are exact in all limits. Similarly for $d = 3$, figure 8 shows equations (65) and (74) plotted and compared. The approximation (74) seems to be quite accurate. Comparison of figure 8 and figure 6 also shows that the convergence of (65) for the dipole only contributions is faster than that obtained by the use of the full contributions as given by (40), even when the interactions due to the charges have been included in the latter⁴.

⁴ Equation (65) has been written in terms of $\bar{\omega}, \bar{p}, \bar{\beta}$ etc by applying the simple transformation $\omega \rightarrow 1/\omega = \bar{\omega}$.

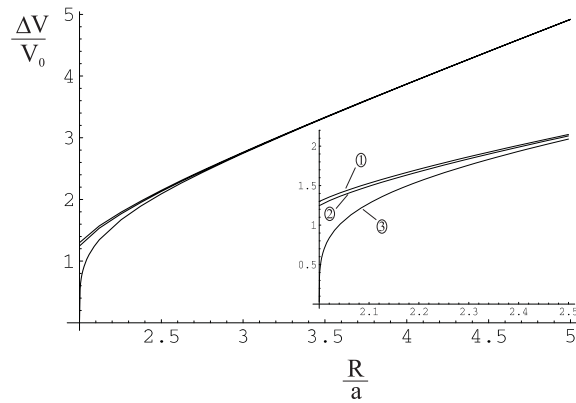


Figure 6. The voltage between two inclusions is shown for the case $d = 3$. The three curves that are shown are (i) the result obtained from (40) *without* the charge contributions (curve 1), (ii) the results from (40) *with* the charge contributions (curve 2) and (iii) the approximation (74) (curve 3). The inset shows the interval $\bar{\omega} \in [2, 2.5]$ so that the convergence can be better differentiated between each case.

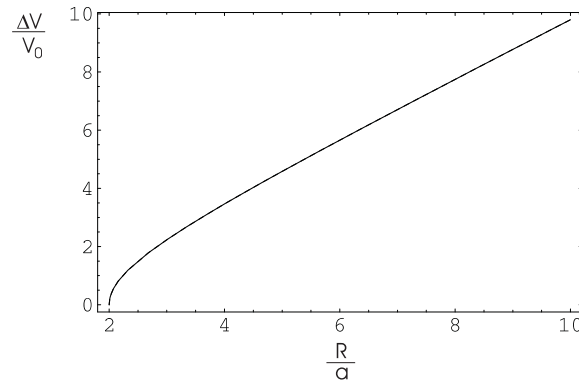


Figure 7. The potential difference is plotted between the two inclusions for $d = 2$. Equations (40), (73) and (65) have the same convergence and thus all the solutions are exact which means that all curves are the same.

$$\frac{\Delta V}{V_0} = \frac{R}{a} - \left(\frac{2}{V_0 \Omega_d a^{d-1}} \right) \left\{ 2^{d-1} \pi E_0 a^d \bar{\omega}_1^{d-1} + 2^{d-1} \pi E_0 a^d \bar{\beta}^{d-1}(\bar{\omega}) \prod_{k=1}^{\gamma} \bar{\omega}_k^d \right. \\ \left. \times \left[1 + \sum_{j=1}^{\gamma} \bar{\beta}^{jd}(\bar{\omega}) \right] + \sum_{n=2}^{\gamma} \bar{\omega}_n^{d-1} \bar{p}_n \right\}. \tag{65}$$

Equation (65) not only reduces the enormous number of terms that need to be calculated as well as reducing computational time for example, it also allows the potential difference between the hyperspheres to be written in terms of closed form polynomial expressions. For instance an approximation for the voltage in $d = 2$ becomes

$$\frac{\Delta V}{V_0} \approx -2 \left[\frac{\delta}{\zeta^2} + \frac{1}{\zeta^2} \sum_{j=8}^{13} \bar{\omega}^{1-2j} \right], \tag{66}$$

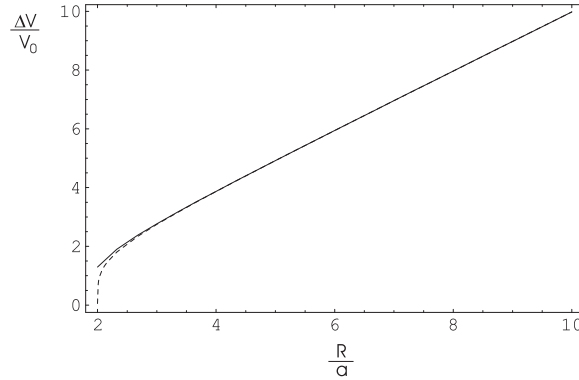


Figure 8. The potential difference is plotted between the two inclusions for $d = 3$. Equations (74) (dashed curve) and (65) (solid curve) show excellent agreement given that (74) is an approximation. However as the two hyperspheres approach each other we find that (65) has not converged to zero. This is because the results plotted do not include the charge contributions which would help convergence to the expected limit more rapidly. Even though the charges have not been included, we see that the convergence is considerably faster than (40) which includes both images and charges, and with a substantially less number of terms required, see also figure 6.

where

$$\delta = -\frac{1}{2\bar{\omega}^{13}}(\bar{\omega}^{14} - 14\bar{\omega}^{12} + 78\bar{\omega}^{10} - 220\bar{\omega}^8) - \frac{1}{2\bar{\omega}^{13}}(330\bar{\omega}^6 - 252\bar{\omega}^4 + 84\bar{\omega}^2 - 8), \quad (67)$$

and

$$\zeta = \frac{1}{\bar{\omega}^6}(\bar{\omega}^6 - 6\bar{\omega}^4 + 10\bar{\omega}^2 - 4). \quad (68)$$

The fact that the potential difference has been written as a polynomial of the n th degree in (66), can be attributed to the properties of the ω_n . Recall that ω_n is written in terms of complicated continued fractions as $n \rightarrow \infty$:

$$\omega_n = \frac{\omega}{1 - \omega\omega_{n-1}}, \quad (69)$$

which can be written down as a polynomial series

$$\omega_n = \sum_{k=0}^{\infty} \omega^{k+1} \omega_{n-1}^k, \quad (70)$$

where (70) is a type of recurrence relation. For example, if $w_1 \equiv w = a/R$ then we obtain w_2 as the polynomial

$$\omega_2 = \omega + \omega^3 + \omega^5 + \omega^7 + \dots, \quad (71)$$

to the desired accuracy after truncating the series. These results allow us to find an approximation for the d -dimensional voltage in terms of a closed form solution in the next section.

6.1. An approximation for the d -dimensional potential difference

The analysis that has been presented in previous sections allows the study of the all important leading terms between the interacting hyperspheres. Using regression techniques we can

obtain a useful approximation for ΔV that can be written down for all dimensions d , as a function of $\bar{\omega} = R/a$. Thus, the d -dimensional potential difference between the hyperspheres is given by the approximation

$$\frac{\Delta V}{V_0} = [\bar{\omega}^{(d-2)}(\bar{\omega}^d - 2^d)]^{\frac{1}{2(d-1)}}. \quad (72)$$

When we consider the $d = 2$ case, (72) simplifies to

$$\frac{\Delta V}{V_0} = [(\bar{\omega}^2 - 4)]^{\frac{1}{2}}. \quad (73)$$

This result is exact in two dimensions to that obtained by Djordjević *et al* [24], who obtained their version by the use of hyperbolic series. In three dimensions the voltage reduces to

$$\frac{\Delta V}{V_0} = [\bar{\omega}(\bar{\omega}^3 - 8)]^{\frac{1}{4}}. \quad (74)$$

Equation (72) can serve as a useful beginning to further investigate the behaviour of the voltage between two hyperspheres with a possible view to resumming otherwise complex terms.

7. Discussion

We have obtained solutions to second order for hyperspherical inclusions using the method of images. The results agree in the various limits with those obtained by others, e.g., for $d = 2$ with Djordjević *et al* [24] and for the case $d = 3$ with Jeffrey [16]. Furthermore, our results using d -dimensional dipole moments means that the convergence is much faster than the multipole expansion method [22]. An interesting extension to the work so far is to try and reproduce these results using a bi-spherical coordinate system in d dimensions, a task that is unfortunately not so easy, given that the solution to $d = 3$ is extremely complicated on its own anyway. In this paper amongst other things, the interaction terms have been resummed so that one-body EMT can be improved and to gain an insight as to how we can extend these results to a many-body EMT. At the same time our study of hyperspheres is important in the areas of topology and geometry [30]⁵. Studies of the surface area and volume have been made with regards to d -dimensional spheres. The results of this paper are useful to such studies since we can write the surface area of a hypersphere as

$$S_d = a^{d-1} A_d, \quad (75)$$

and its volume as

$$V_d = \int a^{d-1} A_d da, \quad (76)$$

where A_d is the surface area of a sphere of radius one and a is the general radius. From here we can study the packing densities of hyperspheres which are paramount in the design of new materials. We are interested in such things as the number of hyperspheres that can ‘touch’ each other in a stable configuration—this is the so-called kissing number. The other important aspect that our results allow us to examine is the virial expansion for the dielectric function:

$$\varepsilon = \varepsilon_0(1 + [\varepsilon]c + \kappa c^2 + O(c^3)). \quad (77)$$

The question we ask is whether (77) does in fact converge to the required results or diverges or if in fact there is any convergence at all. We know that for $d = 1$ and $d = \infty$ the results presented in this paper make EMT exact and by generalizing to d -dimensions we check for

⁵ One must be cautious with regards to the definitions between topology and geometry. These two areas discuss the same problem but the notation is different causing much confusion.

divergence issues⁶. The case $d = 1$ and $d = \infty$ can be thought of as bounds where the true convergence happens to be inside these limits. This is analogous to the variational bounds approach as applied to a composite medium which states that no matter how good any theory is for obtaining the dielectric function, it will always lie between these bounds given as

$$\epsilon_1 + \frac{\epsilon_1 \eta_1}{\frac{\epsilon_1}{(\epsilon_2 - \epsilon_1)} + \frac{\eta_1}{d}} < \epsilon_{\text{eff}} < \epsilon_2 + \frac{\epsilon_2 \eta_1}{\frac{\epsilon_2}{(\epsilon_1 - \epsilon_2)} + \frac{\eta_2}{d}}, \quad (78)$$

and are the so-called Hashin–Shtrikman bounds [31] when we substitute $d = 3$ in (78), where ϵ_i is the dielectric constant for inclusion i and volume fraction η_i . This means that these are the best bounds we are able to obtain. Divergence problems are tackled in statistical mechanics by varying d because these occur due to large fluctuations close to certain dimensions. Furthermore, in some cases, these can have experimental relevance since for systems of infinite degrees of freedom, when these are integrated out, they can sometimes take the form of higher dimensional fluctuations. The classic example is fractals where the proper description of a line for instance is in fact through fractional dimensions. To clarify this a bit more, consider the situation of spheres immersed in a liquid say, then by integrating out the hydrodynamic degrees of freedom, you may have spheres that behave like hyperspheres to a first approximation. This is because the interactions of the fluid and the spheres can be mimicked by interactions in hyperspace. We imagine a $d = 1$ space with a fluid between particles. The effect of the fluid particles can induce interactions that look like higher dimensional interactions. No one has yet however classified all such cases and it is a very interesting area of research. It is hoped that this paper will shed some light in that direction too.

8. Conclusion

We have generalized the interactions between two hyperspheres in a medium in terms of a d -dimensional framework to any order n that has allowed us to obtain the dielectric function for the system. Furthermore, the property of continued fractions has meant that we can resum the otherwise enormous number of complex terms appearing in the interactions, so that only a few orders are necessary in order to obtain the required convergence for the d -dimensional potential difference. Calculations in all limits compare very well with the results of others.

Acknowledgment

The author would like to thank Dr Andrew Shaw for helpful comments and suggestions.

Appendix. The theory of continued fractions

In this section we discuss some of the properties of continued fractions that were used in this paper. We will only cover the basics as a more detailed treatment can be found in any mathematics text, see for example [32]. Suppose we want to evaluate the continued fraction of a number to order n . For integers $b_0, b_1, b_2, \dots, b_n$ we assume that $b_k > 0$ for $k > 0$. These

⁶ Note that as $d \rightarrow \infty$, the charge and dipole contributions tend to zero, since the ratio $\omega = a/R$ which appears in them contains powers of d and $a < R$.

integers can be written down as ratios represented by the notation $\{b_0, b_1, b_2, \dots, b_n\}$ where b_0 is the initial term and is taken to be zero in this paper:

$$\{b_0, b_1, b_2, \dots, b_n\} = b_0 + \frac{1}{b_1 + \frac{1}{b_2 + \dots + \frac{1}{b_n}}}. \quad (\text{A.1})$$

As an example, consider $n = 3$; $b_0 = 2$; $b_1 = 3$; $b_2 = 1$; $b_3 = 4$ so that from (A.1) we obtain

$$\{2, 3, 1, 4\} = 2 + 1/[3 + 1/(1 + 1/4)] = \frac{43}{19}. \quad (\text{A.2})$$

For a continued fraction x of order n , we can find an approximating fraction for x of order $k < n$ such that the continued fraction terminates at the k th denominator. It is obvious that the continued fraction of order k can be written as an ordinary fraction. We therefore have

$$\{b_0, b_1\} = b_0 + 1/b_1 = (b_0 b_1 + 1)/b_1 = \frac{A_1}{B_1} \quad (\text{A.3})$$

$$\{b_0, b_1, b_2\} = b_0 + 1/(b_1 + 1/b_2) = (b_2(b_0 b_1 + 1) + b_0)/(b_1 b_2 + 1) = \frac{A_2}{B_2} \quad (\text{A.4})$$

$$\begin{aligned} \{b_0, b_1, b_2, b_3\} &= b_0 + 1/[b_1 + 1/(b_2 + 1/b_3)] \\ &= (b_3[b_2(b_0 b_1 + 1) + b_0] + b_0 b_1 + 1)/(b_3(b_1 b_2 + 1) + b_1) \\ &= \frac{A_3}{B_3}, \end{aligned} \quad (\text{A.5})$$

and so on where A_i and B_i are integers. If we consider the continued fraction, say, $\{2, 3, 1, 4, 2, 1, 2\}$, then we can represent the second approximating fraction as $\{2, 3, 1\} = 2 + 1/(3 + 1) = 9/4 = A_2/B_2$. More precisely, by the use of (A.3)–(A.5) we find that $A_1/B_1 = 7/3$, $A_2/B_2 = 9/4$, $A_3/B_3 = 43/19$, $A_4/B_4 = 95/42$, \dots . By mathematical induction, recursion formulae can be established as follows,

$$A_k = b_k A_{k-1} + A_{k-2}; \quad B_k = b_k B_{k-1} + B_{k-2} \quad (\text{A.6})$$

where $A_0 = b_0$, $A_{-1} = 1$, $A_{-2} = 0$, $B_0 = 1$, $B_{-1} = 0$ and $B_{-2} = 1$. In the end when we compare the final fraction with the various approximating fractions we see a direct correlation in that the limit of these approximating fractions progressively tends closer and closer to the final fraction with ever increasing accuracy.

References

- [1] Lorentz H A (reprint) 1952 *Theory of Electrons* (New York: Dover)
- [2] Landauer R 1978 Electrical conductivity in inhomogeneous media *Electrical Transport and Optical Properties of Inhomogeneous Media (Ohio State University, 1977)*, (AIP Conference Proceedings no 40) (New York: American Institute of Physics) pp 2–45
- [3] Cohen R W, Cody G D, Coutts M D and Abeles B 1973 *Phys. Rev. B* **8** 3689–701
- [4] Kittel C 1974 *Introduction to Solid State Physics* 4th edn (New York: Wiley)
- [5] Ashcroft N and Mermin N D 1973 *Solid State Phys.* 539–42
- [6] Pauling L and Wilson E B 1935 *Introduction to Quantum Mechanics* (New York: McGraw-Hill)
- [7] Landau L D and Lifshitz E M 1991 *Quantum Mechanics (Non Relativistic Theory) (Course of Theoretical Physics vol 3)* 3rd edn (Oxford: Pergamon)
- [8] Landau L D, Lifshitz E M and Pitaevskii L P 1984 *Quantum Mechanics (Non Relativistic Theory) (Course of Theoretical Physics vol 8)* (Oxford: Pergamon)
- [9] Stoner E C 1945 *Phil. Mag.* **36** 803–6
- [10] Osborn J A 1945 *Phys. Rev.* **67** 351–6
- [11] Bruggeman D A G 1935 *Ann. Phys.* **24** 636–79

- [12] Reitz J R and Milford F J 1970 *Foundations of Electromagnetic Theory* 2nd edn (Reading, MA: Addison-Wesley)
- [13] Maxwell J C 1873 *Electricity and magnetism* 1st edn (Oxford: Clarendon)
- [14] Einstein A 1906 *A. Phys.* **19** 289–306
- [15] Thorpe M F 1992 *Proc. R. Soc. A* **437** 215–27
- [16] Jeffrey D J 1973 *Proc. R. Soc. A* **335** 355–67
- [17] Kelvin Lord 1848 (see Thompson W *Reprint of Paper on Electrostatics and Magnetism* 2nd edn (London: Macmillan) pp 52–85)
- [18] Kalotas T M, Lee A R, Liesegang J and Alexopoulos A 1996 *Appl. Phys. Lett.* **69** 1710
- [19] Simmons J G 1963 *J. Appl. Phys.* **34** 2581
- [20] Simmons J G 1964 *J. Appl. Phys.* **35** 2472
- [21] Neumann C 1883 *Hydrodynamische Untersuchungen nebst einem Anhang uber die Probleme der Elektrostatik und der magnetischen Induktion* (Leipzig: Teubner) pp 279–82
- [22] Choy T C, Alexopoulos A and Thorpe M F 1998 *Proc. R. Soc. A* **454** 1973–1992
- [23] Choy T C, Alexopoulos A and Thorpe M F 1998 *Proc. R. Soc. A* **454** 1993–2013
- [24] Djordjević B R, Hetherington J H and Thorpe M F 1996 *Phys. Rev. B* **53** 14862–71
- [25] Moussiaux A and Ronveaux J 1979 *J. Phys. A* **12** 423
- [26] Jeffrey D J and Onishi Y 1980 *Proc. R. Soc. A* **13** 2847
- [27] Love J D 1975 *Phil. Mag.* **28** 449
- [28] Batchelor G K and O'Brien R W 1977 *Proc. R. Soc. A* **335** 313
- [29] Lebedev N N, Skalskaya I P and Uflyand Y S 1965 *Worked Problems in Applied Mathematics* (New York: Dover) p 242
- [30] Coxeter H S M 1973 *Regular Polytopes* 3rd edn (New York: Dover)
- [31] Hashin Z and Shtrikman S 1962 *J. Appl. Phys.* **33** 3125–31
- [32] Weisstein E W 1999 *CRC Concise Encyclopedia of Mathematics* (Boca Raton: Chapman and Hall/CRC) pp 315–20